Analysis, Modeling, and Simulation of Phase Noise in Monolithic Voltage-Controlled Oscillators

Behzad Razavi
AT&T Bell Laboratories, Holmdel, NJ07733

Abstract

In this paper, the phase noise of monolithic voltage-controlled oscillators is formulated with the aid of a linearized model. A new definition of Q is introduced and three mechanisms leading to phase noise are identified. A simulation technique using sinusoidal noise components is also described.

I. Introduction

Low-noise voltage-controlled oscillators (VCOs) are an integral part of high-performance phase-locked systems such as frequency synthesizers used in wireless tranceivers. While most present implementations of RF VCOs employ external inductors to achieve a low phase noise, the trend towards large-scale integration and low cost mandates monolithic solutions. For example, ring oscillators have been proposed as a suitable candidate [1], but their phase noise is generally known to be "high."

This paper describes an approach to analyzing, modeling, and simulating the phase noise of monolithic VCOs, with particular attention to CMOS ring oscillators. Following an analysis of a general oscillatory system and a new definition of the quality factor, Q, we employ a linearized model of ring oscillators to predict the phase noise with reasonable accuracy.

II. General Oscillatory System

Consider the linear feedback system depicted in Fig. 1. The system oscillates at $\omega = \omega_0$ if the transfer function

$$\frac{Y}{X}(j\omega) = \frac{H(j\omega)}{1 + H(j\omega)} \tag{1}$$

goes to infinity at this frequency, e.g., $H(j\omega_0) = -1$. (We call ω_0 the "carrier frequency.") The phase noise observed at the output is a function of: 1) sources of noise in the circuit, and 2) how much the feedback system rejects (or amplifies) various noise components. Modeling each source of noise as an input, $X(j\omega)$, to the system, we first quantify the latter effect for frequencies close to ω_0. If $\omega = \omega_0 + \Delta\omega$, then $H(j\omega) \approx H(j\omega_0) + \Delta\omega dH/d\omega$ and the noise transfer function is

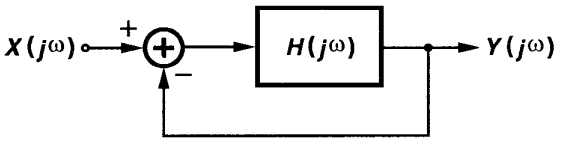

Fig. 1. General oscillatory system.

$$\frac{Y}{X}[j(\omega_0 + \Delta\omega)] = \frac{H(j\omega_0) + \Delta\omega\dfrac{dH}{d\omega}}{1 + H(j\omega_0) + \Delta\omega\dfrac{dH}{d\omega}}. \tag{2}$$

Since $H(j\omega_0) = -1$ and for most practical cases $|\Delta\omega dH/d\omega| \ll 1$, (2) reduces to

$$\frac{Y}{X}[j(\omega_0 + \Delta\omega)] \approx \frac{-1}{\Delta\omega\dfrac{dH}{d\omega}}. \tag{3}$$

This equation indicates that a noise component at $\omega = \omega_0 + \Delta\omega$ is multiplied by $-(\Delta\omega dH/d\omega)^{-1}$ when it appears at the output of the oscillator. In other words, the noise power spectral density is shaped by

$$\left|\frac{Y}{X}[j(\omega_0 + \Delta\omega)]\right|^2 = \frac{1}{(\Delta\omega)^2\left|\dfrac{dH}{d\omega}\right|^2}. \tag{4}$$

This is illustrated in Fig. 2. As we will see later, (4) assumes a simple form for ring oscillators.

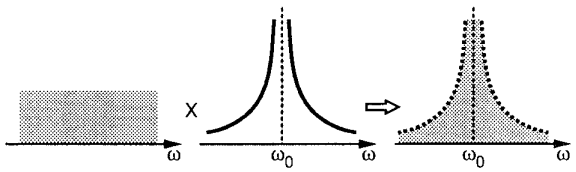

Fig. 2. Noise shaping in oscillators.

To gain more insight, let $H(j\omega) = A(\omega)\exp[j\Phi(\omega)]$. Thus, (4) can be written as

$$\left|\frac{Y}{X}[j(\omega_0 + \Delta\omega)]\right|^2 = \frac{1}{(\Delta\omega)^2[(\dfrac{dA}{d\omega})^2 + (\dfrac{d\Phi}{d\omega})^2]}. \tag{5}$$

0-7803-2584-2/95 $3.00 ©1995 IEEE

We define the open-loop Q as

$$Q = \frac{\omega_0}{2}\sqrt{(\frac{dA}{d\omega})^2 + (\frac{d\Phi}{d\omega})^2}. \quad (6)$$

The *open-loop Q* is a measure of how much the *closed-loop* system opposes variations in the frequency, as is better seen when (5) and (6) are combined:

$$\left|\frac{Y}{X}[j(\omega_0 + \Delta\omega)]\right|^2 = \frac{1}{4Q^2}(\frac{\omega_0}{\Delta\omega})^2, \quad (7)$$

a familiar form previously derived for simple LC oscillators [2]. It is interesting to note that in an LC tank at resonance, $dA/d\omega = 0$ and (6) reduces to the conventional definition of Q: $\omega_0(d\Phi/d\omega)/2$. As will be seen later, in ring oscillators $dA/d\omega$ and $d\Phi/d\omega$ are of the same order and only the more general definition proposed in (6) can be used.

III. Linearized Model of CMOS VCOs

Submicron CMOS technologies have demonstrated potential for RF phase-locked systems [3]. Fig. 3 shows a fully differential 3-stage ring oscillator suitable for such applications. To calculate the phase noise, we model the signal path in the VCO with a linearized (single-ended) circuit as in Fig. 4. Here, R and C represent the output resistance and the load capacitance of each stage, respectively, ($R \approx 1/g_{m3} = 1/g_{m4}$), and G_mR is the gain required for steady oscillations. The noise of each differential pair and its load devices is modeled as current sources I_{n1}-I_{n3}, injected onto nodes 1-3, respectively.

Before calculating the noise transfer function, we note that the circuit of Fig. 4 oscillates if, at ω_0, each stage has unity voltage gain and 120° of phase shift. Thus, $\omega_0 = \sqrt{3}/(RC)$, and $G_mR = 2$, and the open-loop transfer function is given by

$$H(j\omega) = \frac{-8}{(1 + j\sqrt{3}\frac{\omega}{\omega_0})^3}. \quad (8)$$

Therefore, $|dA/d\omega| = 9/(4\omega_0)$ and $|d\Phi/d\omega| = 3\sqrt{3}/(4\omega_0)$. It follows from (5) that if a noise current I_{n1} is injected onto node 1 in the oscillator of Fig. 4, then its power spectrum is shaped by

$$\left|\frac{V_1}{I_{n1}}[j(\omega_0 + \Delta\omega)]\right|^2 = \frac{R^2}{27}(\frac{\omega_0}{\Delta\omega})^2. \quad (9)$$

This equation is the key to predicting various phase noise components in the ring oscillator.

IV. Additive and Multiplicative Noise

Modeling the ring oscillator of Fig. 3 with the linearized circuit of Fig. 4 entails a number of issues. While the stages in Fig. 3 turn off for part of the period, the linearized model exhibits no such behavior. Furthermore, the dependence of the delay upon the tail current I_{SS} is not reflected in Fig. 4. In order to incorporate these effects, we identify three types of phase noise.

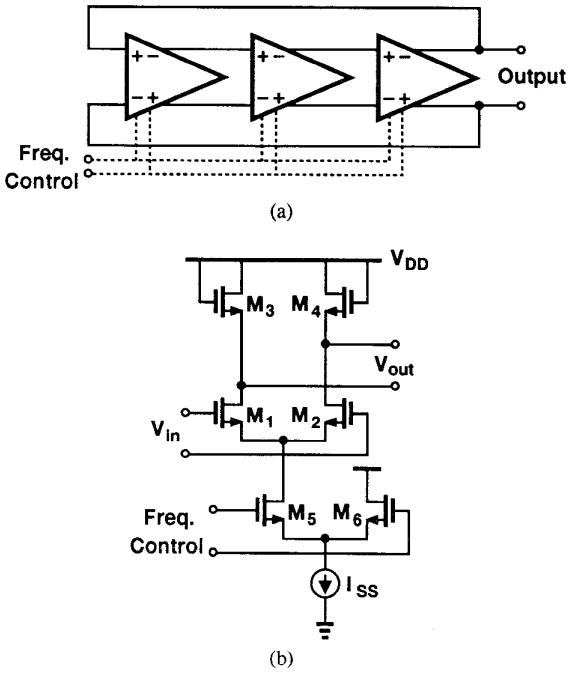

Fig. 3. CMOS VCO. (a) Block diagram, (b) implementation of one stage.

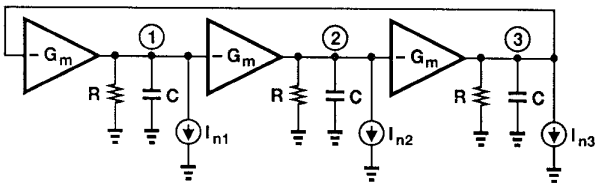

Fig. 4. Linearized model of the VCO.

A. Additive Noise

Additive noise consists of components that are directly added to the output as shown in Fig. 2 and formulated by (4) and (9).

To calculate the additive phase noise in Fig. 4 with the aid of (9), we note that for $\omega \approx \omega_0$ the voltage gain in each stage is close to unity, and the total output phase noise power density due to I_{n1}-I_{n3} is

$$|V_{1tot}[j(\omega_0 + \Delta\omega)]|^2 = \frac{R^2}{9}(\frac{\omega_0}{\Delta\omega})^2\overline{I_n^2}, \quad (10)$$

where it is assumed $\overline{I_{n1}^2} = \overline{I_{n2}^2} = \overline{I_{n3}^2} = \overline{I_n^2}$. For the differential stage of Fig. 3(b), the noise current per unit

bandwidth is equal to $\overline{I_n^2} = 8kT(g_{m1} + g_{m3})/3 \approx 8kT/R$. Thus,

$$|V_{1tot}[j(\omega_0 + \Delta\omega)]|^2 = 8kT\frac{R}{9}(\frac{\omega_0}{\Delta\omega})^2. \qquad (11)$$

Additive phase noise is predicted by the linearized model with high accuracy if the stages in the ring oscillator turn off for only a small portion of the period. In a 3-stage CMOS oscillator designed for the 900-MHz range, the differential pairs turn off for less than 10% of the period. Furthermore, at zero-crossing points —where most of the phase noise is generated— all stages are on. Therefore, the linearized model emulates the CMOS oscillator with reasonable accuracy. A simple measure of this accuracy is the error in the oscillation frequency of the model with respect to that of the actual circuit. This error remains below 10% for a 3-stage ring and 20% for a 4-stage ring.

Since additive noise is shaped according to (11), its effect is significant only for components close to the carrier frequency.

B. High-Frequency Multiplicative Noise

The nonlinearity in the differential stages of Fig. 3, especially as they turn off, causes noise components to be multiplied by the carrier (and by each other). If the input/output characteristic of each stage is expressed as $V_{out} = \alpha_1 V_{in} + \alpha_2 V_{in}^2 + \alpha_3 V_{in}^3$, then for an input consisting of the carrier and a noise component, e.g., $V_{in}(t) = A_0 \cos\omega_0 t + A_n \cos\omega_n t$, the output exhibits the following important components:

$V_{out1}(t) \propto \alpha_2 A_0 A_n \cos(\omega_0 \pm \omega_n)t$,
$V_{out2}(t) \propto \alpha_3 A_0 A_n^2 \cos(\omega_0 - 2\omega_n)t$,
$V_{out3}(t) \propto \alpha_3 A_0^2 A_n \cos(2\omega_0 - \omega_n)t$.

Note that $V_{out1}(t)$ appears in band if ω_n is small, i.e., if it is a *low-frequency* component, but in a fully differential configuration, $V_{out1}(t) = 0$ because $\alpha_2 = 0$. Also, $V_{out2}(t)$ is negligible because $A_n \ll A_0$, leaving $V_{out3}(t)$ as the only significant cross-product.

Simulations indicate that the feedback in the oscillator yields approximately equal magnitudes for $V_{out3}(t)$ and the original component at ω_n. Thus, the nonlinearity folds all the noise components below ω_0 to the region above and vice versa, effectively doubling the noise power predicted by (11). Such components are significant if they are close to ω_0 and are herein called high-frequency multiplicative noise. This phenomenon is illustrated in Fig. 5.

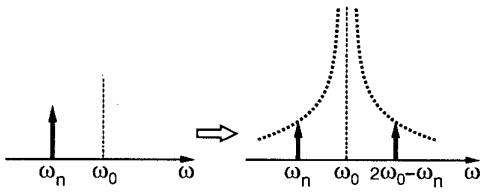

Fig. 5. High-frequency multiplicative noise.

C. Low-Frequency Multiplicative Noise

Since the frequency of oscillation in Fig. 3 is a function of the tail current in each differential pair, noise components in this current modulate the frequency, thereby contributing phase noise. Depicted in Fig. 6, this effect can be significant because, in CMOS oscillators, ω_0 must be adjustable by approximately $\pm 20\%$ to compensate for process variations, thus making the frequency quite sensitive to noise in the tail current.

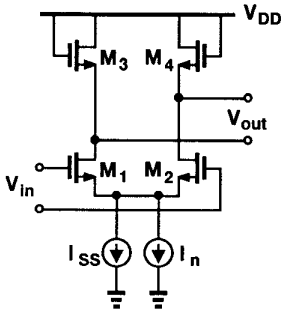

Fig. 6. Carrier modulation by tail noise current.

To quantify this phenomenon, we note that since variations in the tail current modulate the impedance of M_3 and M_4, the resistor R in the linearized circuit can be modeled as the sum of a constant term and a small current-dependent term. It can be proved that if the noise current $I_n = I_{n0}\cos\omega_n t$, then two current components described by $\frac{\sqrt{3}}{4} I_{n0}\cos(\omega_0 \pm \omega_n)t$ appear in the signal path and hence are multiplied by the transfer function in (9). Thus,

$$|V_n|^2 = \frac{R^2}{48}(\frac{\omega_0}{\Delta\omega})^2 |I_n|^2, \qquad (12)$$

where $\Delta\omega = \omega_n$. This mechanism is illustrated in Fig. 7.

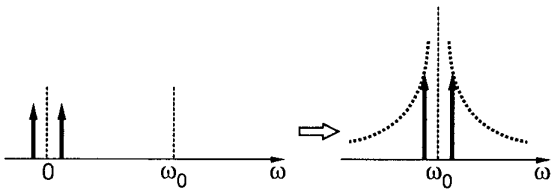

Fig. 7. Low-frequency multiplicative noise.

It is seen that modulation of the carrier brings the low frequency noise components of the tail current to the band around ω_0. Thus, flicker noise in I_n becomes particularly important.

In the differential stage of Fig. 3(b), two sources of low-frequency multiplicative noise can be identified: noise in

I_{SS} and noise in M_5 and M_6. For comparable device size, these two sources are of the same order and must be both taken into account.

V. Simulation

To simulate the phase noise in the oscillator and verify the accuracy of the above derivations, we use a small sinusoidal "noise" current that is injected onto different nodes of the circuit. This approach is justified by the fact that random noise can be expressed as a Fourier series of sinusoids with random phase [4].

Designed to operate at 970 MHz, each oscillator is simulated in the time domain for 2 μsec with 30-psec steps and the resulting output waveform is processed by Matlab to obtain the spectrum. Shown in Fig. 8 is the output spectrum of the linearized model in response to a sinusoidal current with 2-nA amplitude at 980 MHz. The vertical axis represents $10 \log V_{rms}^2$. The observed magnitude of the 980-MHz component is in exact agreement with (10).

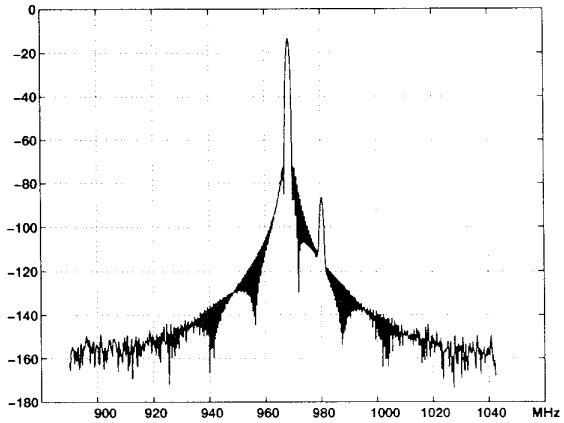

Fig. 8. Simulated spectrum of linearized model.

A similar test on the CMOS oscillator of Fig. 3 yields the spectrum in Fig. 9. Note that the component at 980 MHz has approximately the same magnitude as that in Fig. 8, indicating that the linearized model is indeed an accurate representation. As explained in Section IV, the 960-MHz component originates from third-order mixing of the carrier and the 980-MHz component and essentially doubles the phase noise.

Low-frequency multiplicative noise is simulated by modulating the tail current of one stage in the CMOS oscillator with a 2-nA 10-MHz sinusoid. The resulting sideband magnitudes, shown in Fig. 10, closely agree with (12).

VI. Conclusion

Analysis of a general oscillatory system leads to a linearized model of ring oscillators that predicts the phase noise with reasonable accuracy. Quantified in this paper are three mechanisms, namely, additive noise, high-frequency multiplicative noise, and low-frequency multiplicative noise, that contribute to the phase noise of oscillators. Simulations confirm the accuracy of the model and the derivations.

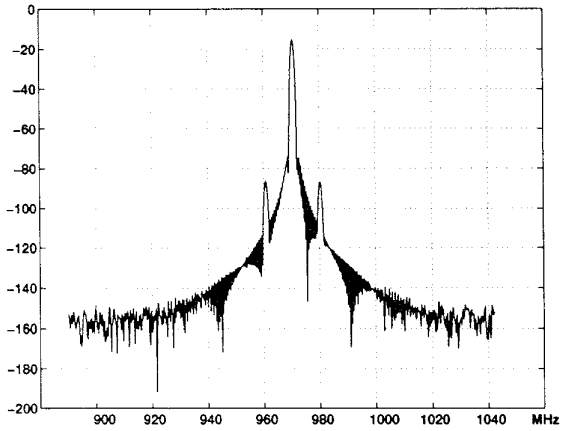

Fig. 9. Simulated spectrum of CMOS VCO.

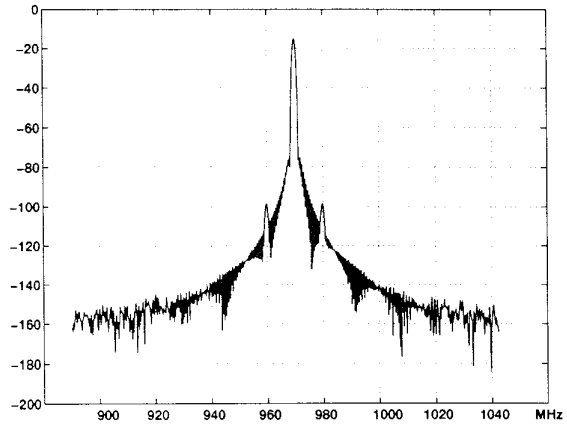

Fig. 10. Simulated spectrum of CMOS VCO with tail current noise.

References

[1] A. A. Abidi, "Radio-Frequency Integrated Circuits for Portable Communications," *Proc. CICC*, pp. 151-158, May 1994.

[2] D. B. Leeson, "A Simple Model of Feedback Oscillator Noise Spectrum," *Proc. IEEE*, pp. 329-330, Feb. 1966.

[3] B. Razavi, "A 3-GHz 25-mW CMOS Phase-Locked Loop," *VLSI Circuits Symp. Dig. Tech. Papers*, pp. 131-132, June 1994.

[4] S. O. Rice, "Mathematical Analysis of Random Noise," *Bell System Tech. J.*, pp. 282-332, July 1944, and pp. 46-156, Jan. 1945.